INFORMATICS JOURNALS
The Journal of Electrochemical Society of India, Volume 75, Issue (1&2), January-March 2026; pp. 67–77
ISSN (Print) : 0013-466X
ISSN (Online) : xxxx-xxxx
DOI: 10.18311/JESCI/2026/56111

Properties of Electrodeposited Ni Composite Coating Containing Synthesised and Washed $ZnAl_2O_4$ Powder

S. Venkatavaradan and S. T. Aruna*

Surface Engineering Division, Council of Scientific and Industrial Research-National Aerospace Laboratories, HAL Airport Road, Bangalore - 560017, India

Abstract

In this study, the effect of particle pretreatment on the properties of electrodeposited Ni-$ZnAl_2O_4$ composite coating is investigated. When attempts were made to codeposit as synthesised $ZnAl_2O_4$ particles from the solution combustion method from a nickel sulfamate bath, a black-coloured solar-selective coating was obtained. The composition of the black coating indicated the formation of a Ni-Zn alloy coating, and no particles were incorporated into the coating and did not result in the formation of a Ni-$ZnAl_2O_4$ composite coating. This was attributed to the presence of zinc salt on the powders, as the powders were neither calcined nor washed after the solution combustion reaction. However, after using the $ZnAl_2O_4$ powder that was washed and dried, Ni-$ZnAl_2O_4$ composite coatings were achieved. The Ni-$ZnAl_2O_4$ coatings were obtained at various applied current densities. The coating electrodeposited at 0.75A/dm^2 showed a microhardness of 429 KHN. In general, microhardness values decreased with increasing applied current density. The variation of corrosion resistance of the coatings with respect to applied current density is reported. The wear resistance of the coating that exhibited better corrosion resistance was also evaluated.

Keywords: Corrosion, Electrodeposited, Microhardness, Ni, Wear, $ZnAl_2O_4$

1. Introduction

Metal Matrix Composite (MMC) coatings containing insoluble reinforcing fillers in the pure metal or alloy matrices are in great demand as they exhibit improved properties when compared to the pure metal/alloy matrices[1-5]. Only a few methods like powder metallurgy, electrodeposition, electroless deposition, *etc.*, are suited for developing such composites. Among the many types of MMCs, electrodeposited composites are very attractive as they are very cost-effective and easy to mass produce. The main application areas of the composite coatings are in engineering applications including automobile and aerospace industries. Among the different electrodeposited metal matrix coatings, Ni composite coatings are propitious coatings as they exhibit improved microhardness, wear resistance and corrosion resistance compared to plain Ni coating[5-36]. A few seminal review articles have highlighted all aspects of electrodeposited metal matrix coatings[24,29,30,33,34,36,37].

The properties of the MMCs are dictated by the volume fraction of particles incorporated in the matrix. The volume fraction of particles incorporated in the MMCs is dependent on the particle size, shape, particle size distribution, bath composition and the plating parameters. The particle properties are dependent on the method used for the synthesis of the particles. The particles are chosen based on the envisaged properties of the composite. Particle mass transfer and the particle-electrode interaction depend on the particle density. Denser particles tend to settle in the bath and hence, the particles should not be too large. Generally, particles ~1 μm are desirable for codeposition. A decrease in the specific surface area increases the incorporation of

*Email: aruna_reddy.nal@csir.res.in

particles and the surface area is in turn, determined by the shape of particles. Furthermore, the mechanism of codeposition of particles in the electrodeposited metal matrix has been well documented in literature[29].

The bath composition dictates the properties of the coating and important bath parameters include the constituents, aging, pH and additives. Many of these aspects have been studied by researchers across the globe. A large number of filler particles, such as ceramic particles, microcapsules, carbon nanotubes, diamond particles, *etc.*, have been used as dispersed phase in the Ni metal matrix composite coatings[5-36]. A large number of ceramic particles like Al_2O_3, ZrO_2, TiO_2, CeO_2, *etc.*, have been incorporated into Ni matrix and the effect of various parameters on the properties of the composite coatings have been reported. Researchers continue to report Ni composite coatings containing newer particles like TiC, carbon black, rGO, *etc.*[7,10,11]. The authors` group has explored a large number of particles like YSZ, PSZ, alumina, ceria, yttria doped ceria, yttria zirconia alumina, oil-containing microcapsules, pumice, cenosphere, *etc.*, as distributed phases in electrodeposited Ni composite coatings and reported improved microhardness, wear resistance and corrosion resistance compared to plain Ni coating[12-26].

To date, $ZnAl_2O_4$ has not been explored as a reinforcement in electrodeposited Ni composite coatings. Spinel $ZnAl_2O_4$ is a wide energy bandgap (Eg) ceramic oxide material, is also known as gahnite. It finds applications in sensors, photocatalyst, supercapacitor, biosensor, electroconductive material, *etc*[28-30]. $ZnAl_2O_4$ exhibits a high mechanical resistance, fluorescence efficiency, photocatalytic activity and chemical and thermal stability[39-40]. It also exhibits low surface acidity.

In the present study, an attempt is made to synthesise $ZnAl_2O_4$ powder and codeposit it into the Ni metal matrix. $ZnAl_2O_4$ powder was prepared by Solution Combustion Synthesis (SCS). SCS is a simple, cost-effective and versatile method[41]. The microhardness, wear resistance and corrosion resistance of the Ni-$ZnAl_2O_4$ coatings are reported.

2. Experimental

2.1 $ZnAl_2O_4$ Powder Synthesis by the Solution Combustion Method and Characterisation

Phase pure $ZnAl_2O_4$ powder was synthesised by the solution combustion method as follows: An aqueous redox mixture containing 100 g of aluminium nitrate (Merck), 29.255 g of zinc acetate (Loba Chemie) and 53.32 g of urea (Merck) in a minimum amount of distilled water was prepared and stirred well, followed by heating the solution on a preheated hot plate. The solution underwent flame-type combustion, yielding a white voluminous $ZnAl_2O_4$ powder. The obtained powder was crushed with the help of a pestle and mortar and used for electrodeposition.

2.2 Preparation of Nickel-zinc Aluminate Coatings

A 200 mL Ni-sulfamate bath containing 20 g of zinc aluminate powder was taken in a glass beaker and stirred for 16 hours before electrodeposition. Electrodeposition was carried out at 0.75, 1.54, 3.1 and 4.65 A/dm^2, respectively, for 6, 3, 1.5 and 0.52 h, on a magnetic stirrer (400 rpm), so as to obtain the same coating thickness on a 1"x1" area for all the coatings. The schematic of the plating setup used for electrodeposition is shown in Figure 1. Brass pins were also coated for wear tests. During electrodeposition, the solution was stirred at 400 rpm. The pH of the bath was maintained at 4, and electrodeposition was carried out on a polished brass plate for characterisations like microhardness, cross-section, and mild steel substrates for corrosion studies. More details regarding the bath, sample preparation, coating development and characterisation have already been reported by the authors[22,24].

2.3 Characterisation of Coatings

The phase of the as-synthesised $ZnAl_2O_4$ powder was confirmed using a Bruker-Advance D8 X-ray diffractometer with Cu Kα as the radiation source and Ni as the filter. The particle size distribution and average agglomerated particle size of $ZnAl_2O_4$ powder were obtained using a particle size analyser based on the laser light scattering technique (Master sizer 2000, Malvern). The morphology of the particles was recorded using a Field Emission Scanning Electron Microscope (FESEM, Supra 40VP model, Carl Zeiss) integrated with Energy Dispersive X-ray Analyser (EDAX, Gemini column).

The optical properties, such as absorptance (α) and emissivity (ε) of the black colored coatings were measured using a solar spectrum reflectometer and emissometer (Devices and Services). Microhardness measurements were carried out at four different locations on the polished specimen, in which a Ni-$ZnAl_2O_4$ coated

brass coupon was embedded in a Bakelite matrix and metallographically polished using Al_2O_3 slurry, down to 0.05 µm. Optical micrographs were recorded using an optical microscope. Corrosion studies were carried out in a 3.5 wt % NaCl solution in a 3-electrode setup. Wear studies were carried out using a pin-on-disc tribometer. The microhardness measurements were performed at four different locations on the cross-section of each coating on a Buehler Microhardness Tester (Micromet 100) by applying a 50 gF load. Graphs were plotted for the variation of microhardness vs. current density. Optical images of the cross-sections were recorded using a vertical metallurgical microscope to find the incorporated particle shape and its distribution, and volume fraction on the substrate.

CHI 604 2D electrochemical workstation was employed to evaluate the corrosion behaviour of electrodeposited Ni and Ni-$ZnAl_2O_4$ composite coatings on mild steel substrates. The test was carried out in deaerated 3.5 wt% (0.6 M) 200 mL NaCl solution (200 ± 2 mL) using a conventional 3-electrode cell with a 1cm^2 coated mild steel coupon as the working electrode. The Nyquist and Tafel plots were obtained for all the coatings. Wear tests were done on a pin-on-disc tribometer (Ducom wear tester) to understand the tribological behaviour of composite coatings. Wear tests for the Ni-$ZnAl_2O_4$ coated brass pins were carried out using a pin-on-disc tribometer for a track radius of 30 mm at a speed of 200 rpm under a load of 1kg. The relative humidity during the test was found to be 30 at a room temperature of 35°C. All the characterisation details are already detailed in the authors` previous publications[22,24].

3. Results and Discussion

Figure 2 displays the FESEM images of the solution combustion-synthesised $ZnAl_2O_4$ powder. The FESEM shows that particles are flaky and agglomerated. XRD

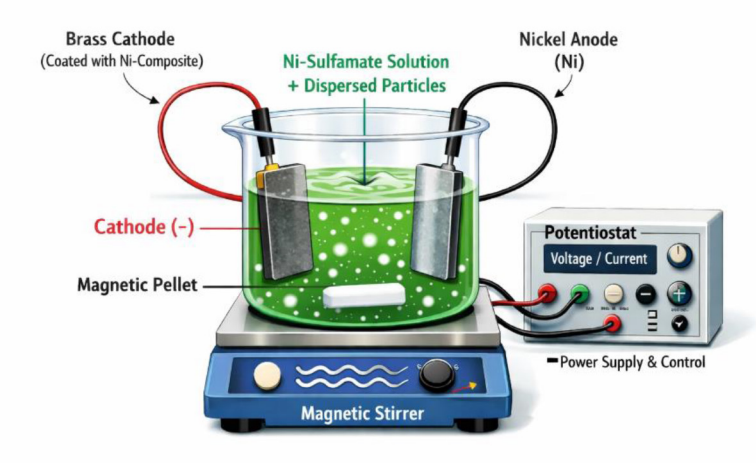


Figure 1. Experimental setup used for electrodeposition of Ni-composite coatings.

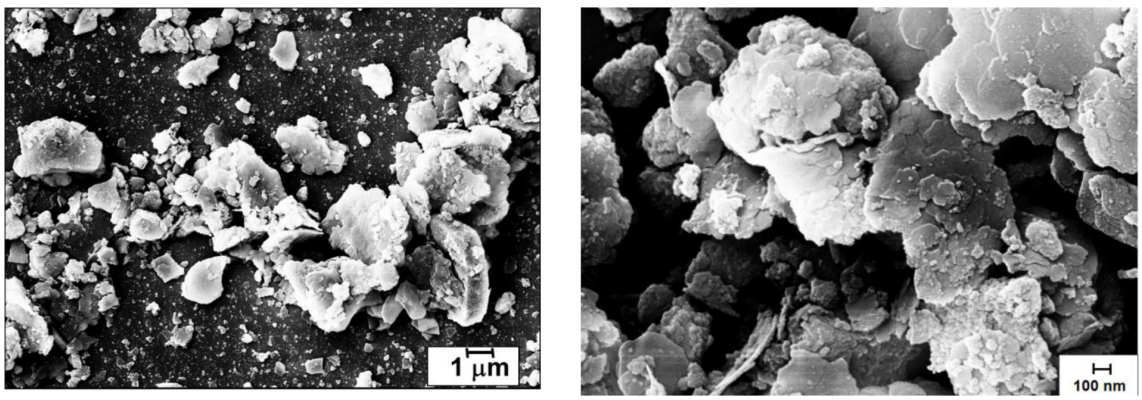


Figure 2. FESEM images of as-synthesised $ZnAl_2O_4$ powder in two different magnifications.

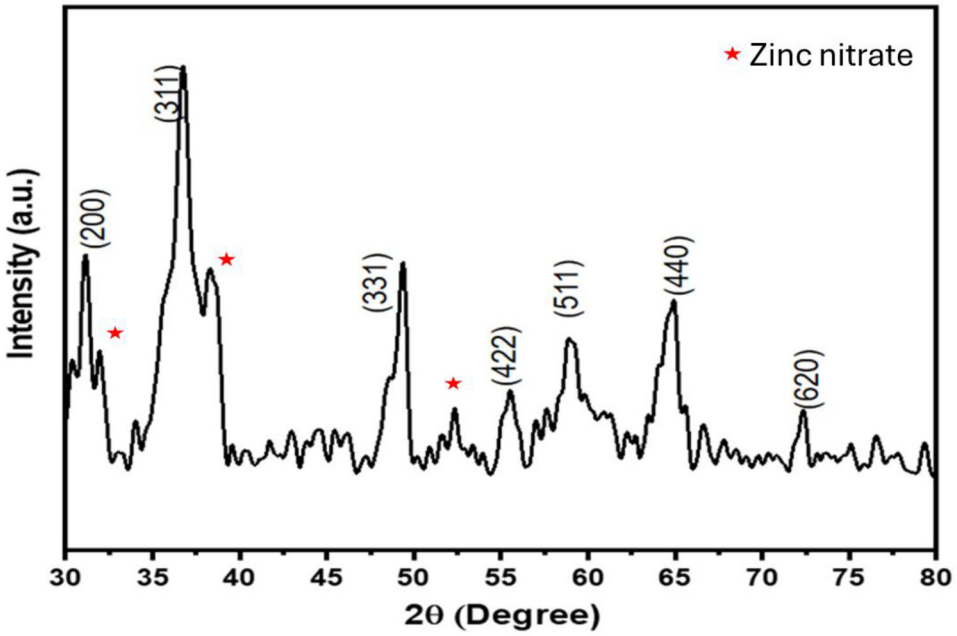


Figure 3. Powder XRD pattern of $ZnAl_2O_4$ powder.

Table 1. Bath and coating details of the Ni-Zn coating, along with its solar selectivity properties

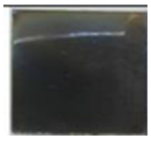
Sample name	$ZnAl_2O_4$ concn (gpL)	Current (A/dm^2)	Plating time	Agitation type/ rpm	Coating	Solar selectivity values
1	100	0.75	30	Magnetic/570		α=0.907 ε=0.540
2	200	0.75	30	Magnetic/570		α=0.752 ε=0.060
3	50	0.75	30	Magnetic/570		α=0.874 ε=0.060
4	80	0.75	30	Magnetic/570		α=0.935 ε=0.560
5	80	0.75	30	Mechanical		α=0.950 ε=0.630
6	80	0.75	15	Mechanical		α=0.926 ε=0.140

Table 2. Potentiodynamic polarisation data of Ni-$ZnAl_2O_4$ coating

Sample@Current density (A/dm²)	Ecorr (V)	Icorr (μA/cm²)	βa (V/dec)	βc (V/dec)	Rp W/cm²
Ni@1.54	-0.414	5.420	4.52	5.25	8195
Ni-$ZnAl_2O_4$@1.54	-0.270	0.087	0.204	0.135	406140
Ni-$ZnAl_2O_4$@3.1	-0.306	0.130	0.227	0.115	254431
Ni-$ZnAl_2O_4$@4.65	-0.304	0.120	0.144	0.111	277963

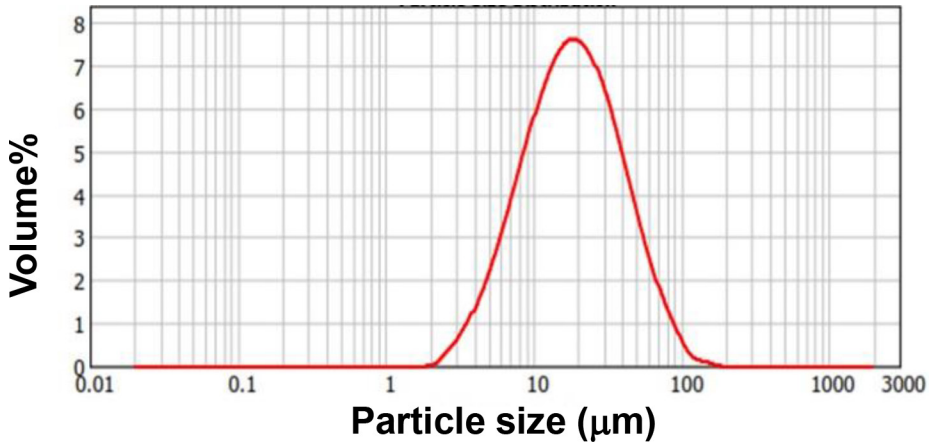


Figure 4. Particle size distribution curve of $ZnAl_2O_4$ powder.

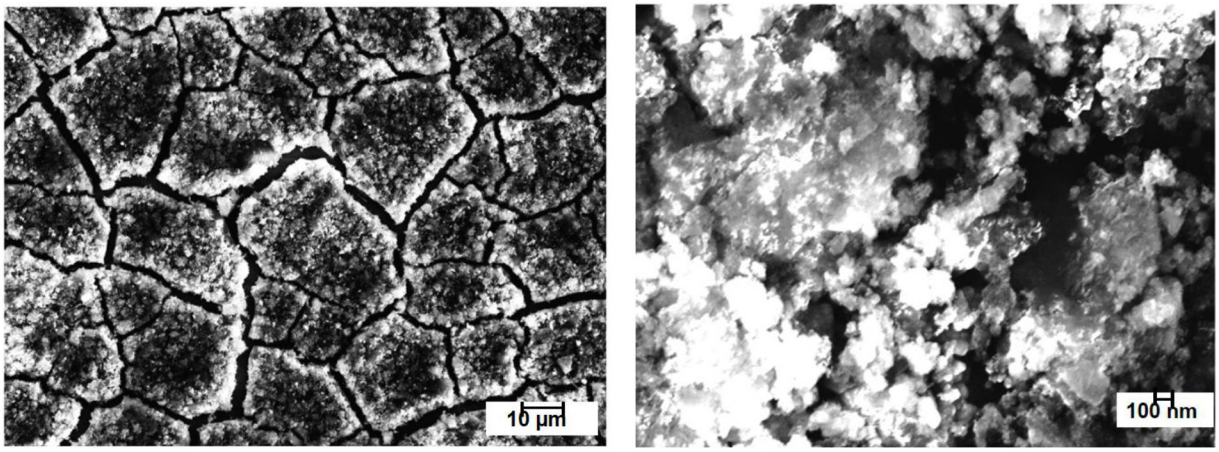
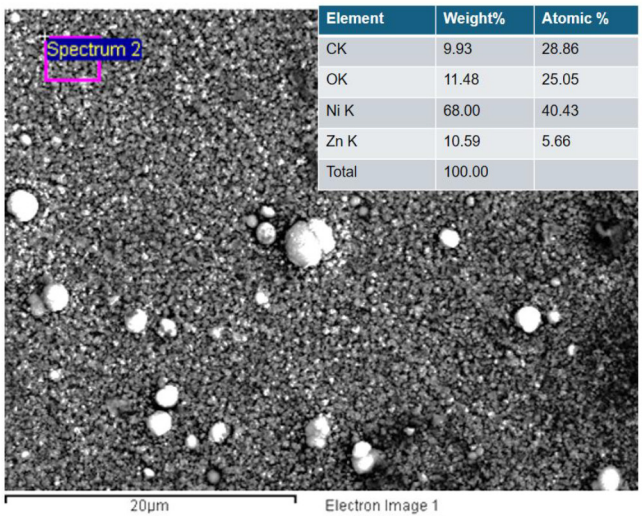


Figure 5. FESEM image of Ni-Zn black coating at two different magnifications.

confirmed that it is a pure zinc aluminate spinel phase (JCPDS no. 05-0669) with some traces of impurities like zinc nitrate (Figure 3). As formed particles were agglomerated, and the average agglomerated particle size was found to be 3.9 μm and showed a very narrow size distribution (Figure 4).

When the as-synthesised $ZnAl_2O_4$ powder was employed as the filler particles, the resulting coating was always black in colour, and no particles were incorporated (Table 1). The FESEM image of the coating is shown in Figure 5; it shows a cracked microstructure and contains nanosized grains. The EDX analysis of the coating showed the presence of Zn and Ni elements (Figure 6). Further, the unburnt Zn salt during SCS was found to be ~10 ppm as determined by atomic absorption spectroscopy. Zn-Ni is also used in solar thermal collectors due to high solar absorptance (up to 0.93) and low emittance. The formation of Ni-Zn coating may be attributed to the presence of unburnt zinc nitrate during SCS. The unburnt zinc nitrate sticking to the particles and on the sides of

the glass beaker as the SCS reaction was carried out on a hotplate, where there is no uniform heating. Generally, in SCS, to maintain uniform heating, the reaction is carried out in a preheated muffle furnace. Further, the reason for not realising the incorporation of $ZnAl_2O_4$ particles along with Ni-Zn may be due to the lack of controlled conditions, such as current density and magnetic stirring speed[42]. The optimal current density for incorporating particles in Ni-Zn alloy may be higher than the current density that was used in the present study, and also the low concentration of Zn ions in the electrolyte bath.



Element	Weight%	Atomic %
CK	9.93	28.86
OK	11.48	25.05
Ni K	68.00	40.43
Zn K	10.59	5.66
Total	100.00	

Figure 6. EDAX data obtained on the black coating.

The volume fraction of particles codeposited in the deposit depends on the applied current density. Optical micrographs (Figure 7) of the Ni- $ZnAl_2O_4$ coatings showed a decrease in the incorporation of filler particles with increasing current densities. At lower current densities, the rate of nickel deposition is lower, and hence a greater number of smaller-sized particles get entrapped in the deposit. As seen from the microhardness plot (Figure 8), microhardness decreases with increasing current density. The highest Knoop microhardness value of ~430 KHN was obtained for the coating electrodeposited at a current density of 0.75A/dm^2. When compared to plain nickel coating, ~100 KHN higher microhardness was observed for the Ni-$ZnAl_2O_4$ coating. This difference is mainly attributed to grain refinement occurring in the case of Ni-$ZnAl_2O_4$ composite coatings.

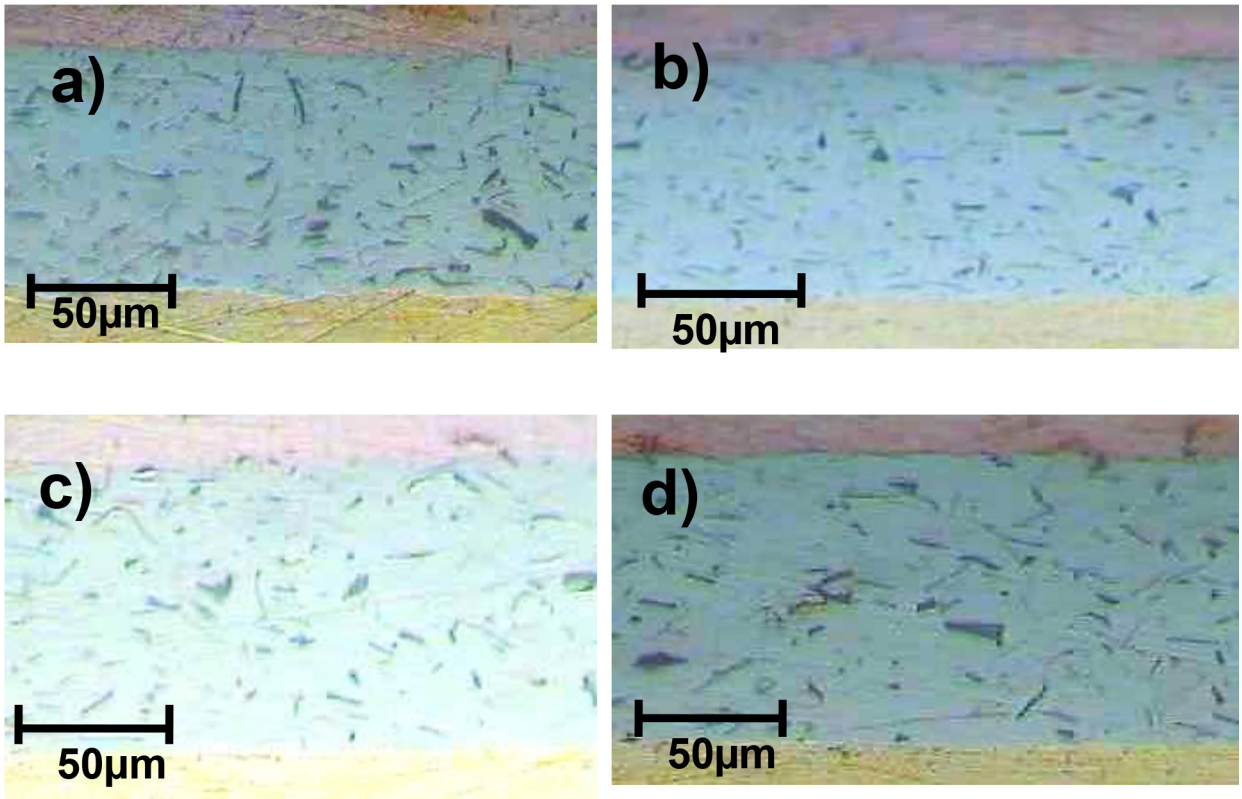


Figure 7. Optical micrographs of Ni-$ZnAl_2O_4$ electrodeposited at **(a)** 0.75A/dm^2 for 6 h, **(b)** 1.54 A/dm^2 for 3 h, **(c)** 3.1 A/dm^2 for 1.5 h and **(d)** 4.65 A/dm^2 for 52 min.

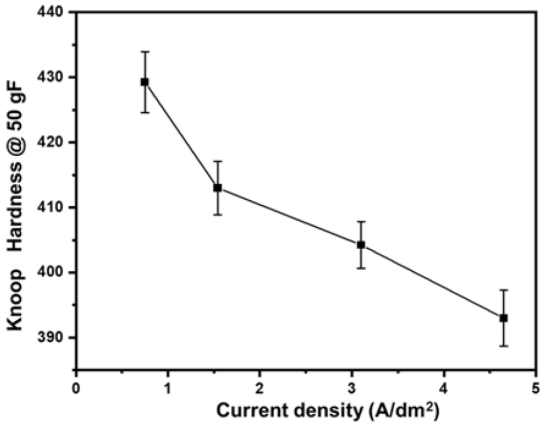


Figure 8. Plot of Knoop microhardness vs. current density of Ni-$ZnAl_2O_4$ coatings.

Using a three-electrode setup, corrosion tests were performed on mild steel substrates coated with Ni-$ZnAl_2O_4$ composite coatings. When compared to the plain nickel, the corrosion current decreased, and the corrosion potential Ecorr (V) values shifted to more positive values when compared to -0.4 V in plain nickel (Table 2). In the case of Ni-$ZnAl_2O_4$ coating, the corrosion resistance was found to be better for the coating electrodeposited at 1.54A/dm^2. It exhibited a corrosion rate of 0.8 x10^{-4} cm/yr.

The observed polarisation resistance values obtained from the Tafel plot (Figure 9a) are substantiated by the Nyquist plots. The coating electrodeposited at 1.54 A/dm^2 shows the highest polarisation resistance and lower icorr

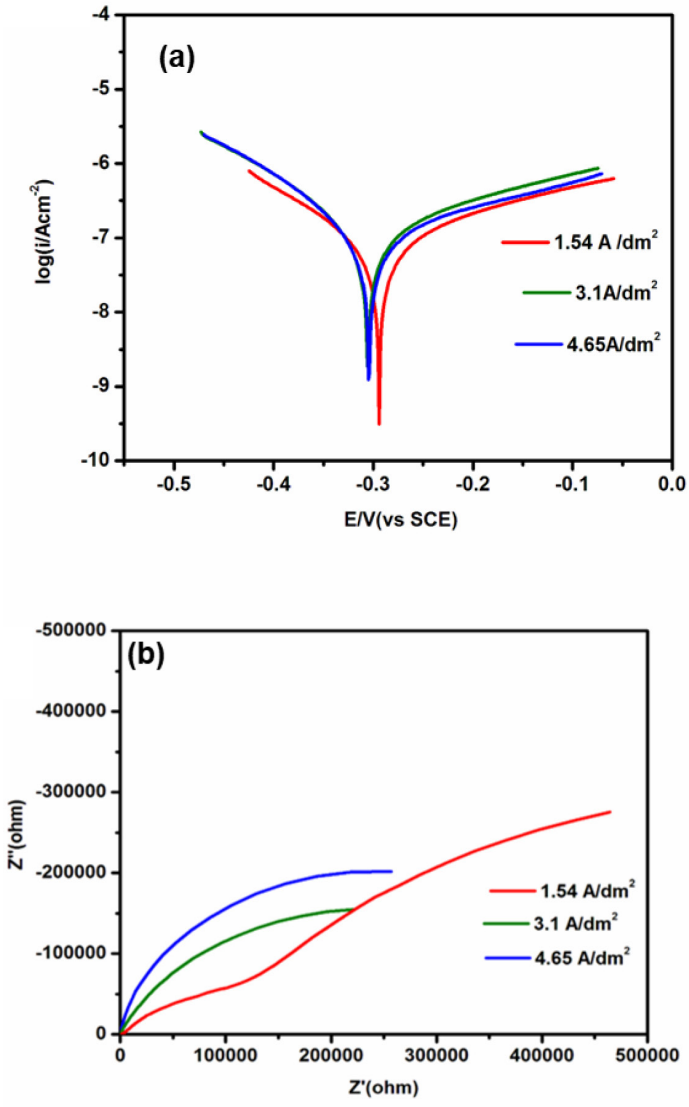


Figure 9. **(a)** Tafel plots and **(b)** Nyquist plots for Ni-$ZnAl_2O_4$ coatings electrodeposited at various current densities.

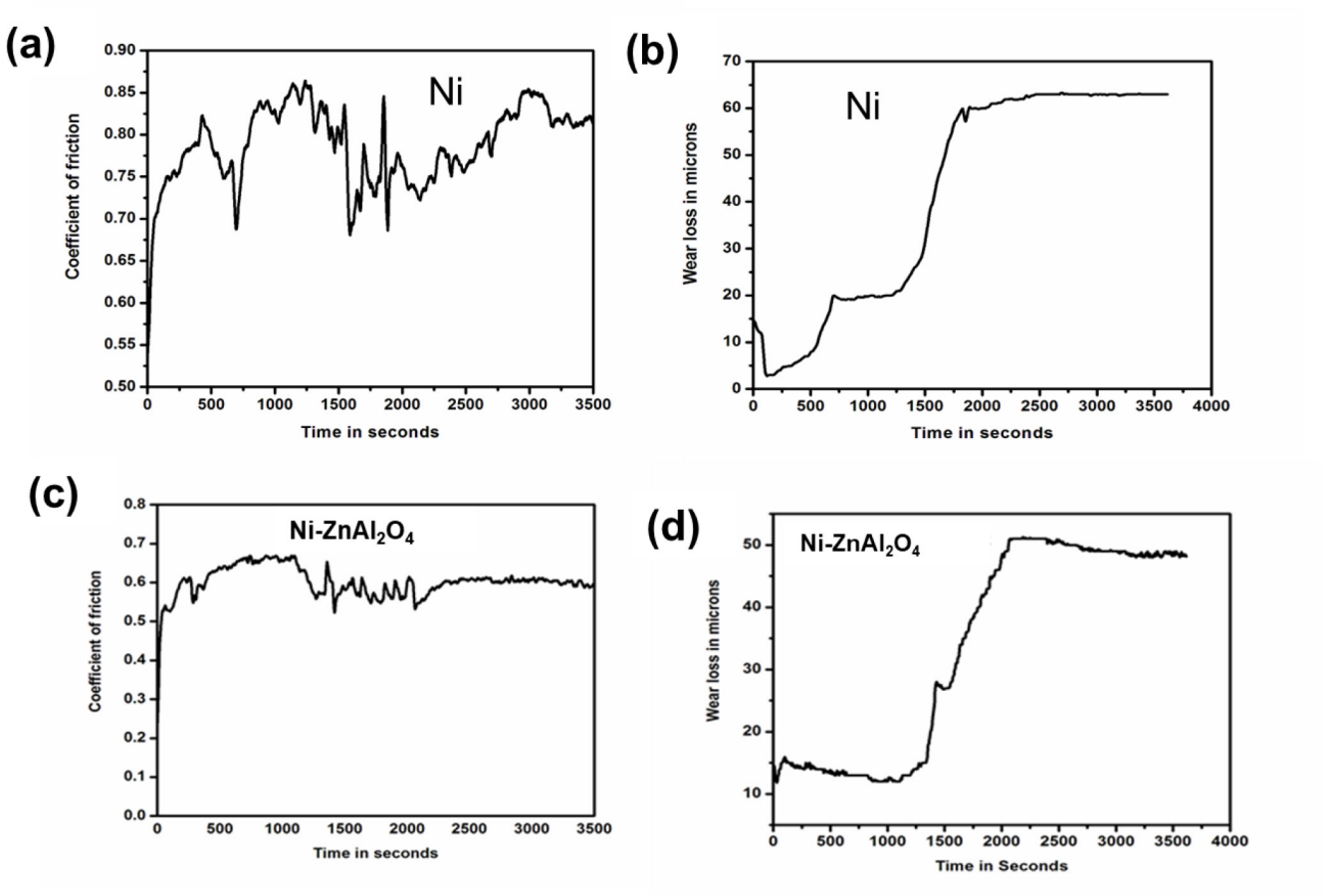


Figure 10. **(a)** Ni coatings - Plots of CoF vs. Time, **(b)** Ni coatings - Wear loss vs. Time, **(c)** Ni-$ZnAl_2O_4$ coatings - Plots of CoF vs. Time, and **(d)** Ni-$ZnAl_2O_4$ coatings - Wear loss vs. Time.

value compared to other coatings. The same coating shows a higher radius of the semicircle in the Nyquist plot (Figure 9b), indicating improved corrosion resistance of the coating.

The optical image of the tested disc showed grooves in the direction of motion of the pins. When compared to the plain Ni, fewer grooves were found in the Ni-zinc aluminate composite coating electrodeposited at 1.54 A/dm^2. The coefficient of friction was found to be lower in the case of Ni-zinc aluminate composite coatings (0.60) compared to 0.75 observed for pure Ni. Further, the coating also showed lower wear loss, indicating improved wear resistance compared to pure Ni coating (Figure 10).

4. Conclusions

The following conclusions can be drawn from this study:

- Zinc aluminate powder prepared by the solution combustion method had some traces of Zn nitrate after SCS.
- Due to this reason, as prepared powders could not be incorporated in the Ni matrix and instead, black colored Zn-Ni coatings exhibiting absorptance values as high as 0.95 and as low as 0.75 were realised. The emittance values as low as 0.060 and as high as 0.63 were achieved.
- Ni-$ZnAl_2O_4$ composite coating was successfully electrodeposited after washing the synthesised powder thoroughly in distilled water and drying in a hot air oven.
- All the electrodeposited Ni-$ZnAl_2O_4$ composite coatings exhibited lower i_{corr} and higher charge resistance (Rct) and polarisation resistance (Rp) values compared to plain Ni, indicating superior improved corrosion resistance.
- Ni- $ZnAl_2O_4$ coating electrodeposited at 1.54 A/dm^2 current density exhibited superior corrosion resistance.
- Ni-$ZnAl_2O_4$ coating electrodeposited at 1.54 A/dm^2 current density exhibited a lower wear rate and lower

coefficient of friction values compared to plain Ni coating.

- Thus, Ni-$ZnAl_2O_4$ coating electrodeposited at the lowest current density exhibited a synergistic combination of higher microhardness, wear resistance and corrosion resistance.
- This study also clearly demonstrated the importance of pretreatment of particles synthesised by the SCS method, either by calcination at temperatures >700 °C or by washing them thoroughly in distilled water before using for composite coating.

5. Acknowledgements

The authors acknowledge the Director, CSIR-NAL, for his encouragement. The authors thank Ms. Ann Miriam for the help received in the electroplating and characterization. The authors also express their gratitude to Mr. Siju and Mr. G. Srinivas for the FESEM and XRD studies. The authors thank Mr. V.K. William Grips for the encouragement and suggestions received during this work.

6. References

1. Nunez M, editor. Metal electrodeposition. New York: Nova Science; 2005.
2. Safavi MS, Walsh FC. The electrodeposition of particle-metal matrix composite coatings to meet tribological and corrosion challenges. Adv Colloid Interface Sci. 2025; 343:103584. https://doi.org/10.1016/j.cis.2025.103584 PMid:40570656
3. Arroyo A, Vásquez FA, Calderón JA. Structural modification of electrodeposited nickel coatings by ceramic particles incorporation to enhance corrosion-erosion resistance. J Mater Res Technol. 2025; 35:7332-7345. https://doi.org/10.1016/j.jmrt.2025.03.086
4. Safavi MS, Tanhaei M, Ahmadipour MF, Adli RG, Mahdavi S, Walsh FC. Electrodeposited Ni-Co alloy-particle composite coatings: A comprehensive review. Surf Coat Technol. 2020; 382:125153. https://doi.org/10.1016/j.surfcoat.2019.125153
5. Samra AS, Zafar S, Ahmad M, Husnain M, Kahraman R, Mansoor B, *et al.* Enhanced mechanical and electrochemical behavior of electrodeposited Ni-B-NbC coatings: Experimental characterization and COMSOL simulation. Mater Sci Eng B. 2026; 327:119222. https://doi.org/10.1016/j.mseb.2026.119222
6. Zhang J, Ma T, Chen D, *et al.* Improving water immersion resistance through optimizing surface energy of reduced graphene oxide (rGO)/nickel composite superhydrophobic coating. MRS Adv. 2026. https://doi.org/10.1557/s43580-025-01525-z
7. Cao M, Tian D, Li C, Wang B, Guo X, Li W, *et al.* Investigation of nozzle angle on the microstructure and abrasion resistance of jet electrodeposited Ni-TiC composites. Sci Rep. 2025; 15:14845. https://doi.org/10.1038/s41598-025-99090-w PMid:40295605 PMCid:PMC12038041
8. Taheri SH, Khazaei BA, Rashidi AM, Boroujerdnia M, Jamali-Sheini F. Effect of co-deposition of TiO_2 and SiC nanoparticles on microhardness, wear and corrosion behavior of electrodeposited Ni-W nanocomposite coating. Mater Chem Phys. 2025; 345:131183. https://doi.org/10.1016/j.matchemphys.2025.131183
9. Zhao Y, Liu S, Guo H, Li H, Zhang J, Ma Z, *et al.* Mechanistic insights on the microstructural evolution and tribological performance of Ni-MoS_2 composite coatings electrodeposited under different current densities. J Mater Res Technol. 2025; 36:8325-8336. https://doi.org/10.1016/j.jmrt.2025.05.055
10. Rao P, Singh S, Kumar K, Pandel U, Srivastava C. Electrochemical behavior and surface chemistry studies of electrodeposited MnMoCrCoFeNiCu high entropy alloy-carbon nanotube composite coatings. J Mater Eng Perform. 2025; 34:3240-3255. https://doi.org/10.1007/s11665-024-09261-5
11. Devesa S, Cavaleiro D, Santo D, Gavinho S, Cunha AF, Santos P, *et al.* Boric acid-free electrodeposition process and solar-thermal energy conversion of Ni-carbon black nanocomposite coatings. J Mater Res. 2024; 39:3397-3410. https://doi.org/10.1557/s43578-024-01477-4
12. Aruna ST, Kiran A, Shilpa M. Reclamation of thermal power plant waste as a distributed phase in electrodeposited Ni composite coating. Surf Eng. 2019; 35:1042-1047. https://doi.org/10.1080/02670844.2019.1627487
13. Aruna ST, Arunima S, Latha S, Grips VKW. Preparation of oil encapsulated microcapsules and tribological property of Ni composite coating containing them. Mater Manuf Process. 2016; 31:107-111. https://doi.org/10.1080/10426914.2014.973585
14. Aruna ST, Lashmi PG, Seema HM. Effect of additives on the properties of electrodeposited Ni-zircon composite coatings. RSC Adv. 2016; 6:11185-11192. https://doi.org/10.1039/C5RA25119B
15. Aruna ST, Srinivas G. Wear and corrosion resistant properties of electrodeposited Ni composite coating containing Al_2O_3-TiO_2 composite powder. Surf Eng. 2015; 31(9):708-713. https://doi.org/10.1179/1743294415Y.0000000050
16. Aruna ST, Anandan C, Grips VKW. Effect of probe sonication and sodium hexametaphosphate on the microhardness and wear behavior of electrodeposited

Ni-SiC composite coating. Appl Surf Sci. 2014; 301:383-390. https://doi.org/10.1016/j.apsusc.2014.02.087
17. Aruna ST, Roy S, Sharma A, Savitha G, Grips VKW. Cost-effective wear and oxidation resistant electrodeposited Ni-pumice coating. Surf Coat Technol. 2014; 251:201-209. https://doi.org/10.1016/j.surfcoat.2014.04.026
18. Aruna ST, MuniPrakash M, Grips VKW. Effect of titania particle preparation on the properties of Ni-TiO_2 electrodeposited composite coatings. J Appl Electrochem. 2013; 43:805-815. https://doi.org/10.1007/s10800-013-0565-y
19. Aruna ST, Grips VKW. Electrodeposited nickel composite coating containing in-situ nickel impregnated alumina particles. Mater Lett. 2012; 66:141-144. https://doi.org/10.1016/j.matlet.2011.08.065
20. Aruna ST, EzhilSelvi V, Grips VKW, Rajam KS. Corrosion and wear resistant properties of Ni-Al_2O_3 composite coatings containing various forms of alumina. J Appl Electrochem. 2011; 41:461-468. https://doi.org/10.1007/s10800-011-0256-5
21. Aruna ST, Grips VKW, Rajam KS. Synthesis and characterization of Ni-Al_2O_3 composite coatings containing different forms of alumina. J Appl Electrochem. 2010; 40:2161-2169. https://doi.org/10.1007/s10800-010-0198-3
22. Aruna ST, Grips VKW, Rajam KS. Ni-based electrodeposited composite coating exhibiting improved microhardness, corrosion and wear resistance properties. J Alloys Compd. 2009; 468: 546-552. https://doi.org/10.1016/j.jallcom.2008.01.058
23. Aruna ST, Grips VKW, EzhilSelvi V, Rajam KS. Synthesis and properties of electrodeposited nickel/yttria doped ceria nanocomposite coatings. J Appl Electrochem. 2007; 37:991-997. https://doi.org/10.1007/s10800-007-9338-9
24. Aruna ST, Bindu CN, EzhilSelvi V, Grips VKW, Rajam KS. Synthesis and properties of electrodeposited Ni/ceria nanocomposite coatings. Surf Coat Technol. 2006; 200:6871-6876. https://doi.org/10.1016/j.surfcoat.2005.10.035
25. Aruna ST, Diwakar S, Jain A, Rajam KS. Comparative study on the effect of current density on Ni and Ni-Al_2O_3 nanocomposite coatings produced by electrolytic deposition. Surf Eng. 2005; 21(5):209-214. https://doi.org/10.1179/174329405X50037
26. Aruna ST, Rajam KS. Synthesis, characterisation and properties of Ni/PSZ and Ni/YSZ nanocomposites. Scr Mater. 2003; 48:507-512. https://doi.org/10.1016/S1359-6462(02)00498-0
27. Guan T, Zhang N. Recent advances in electrodeposition of nickel-based nanocomposites enhanced with lubricating nanoparticles. Nanomanuf Metrol. 2024; 7:25. https://doi.org/10.1007/s41871-024-00245-6 PMid:39679139 PMCid:PMC11638300
28. Gültekin D. Optimizing TiN content in electrodeposited Ni-B-W composite coatings: Microstructure, microhardness, and dry-sliding tribology. J Mater Eng Perform. 2026; 35:11186-11197. https://doi.org/10.1007/s11665-026-13457-2
29. Walsh FC, Wang S, Zhou N. The electrodeposition of composite coatings: Diversity, applications and challenges, Curr Opi Electrochem. 2020; 20:8-19. https://doi.org/10.1016/j.coelec.2020.01.011
30. Zellele DM, Yar-Mukhamedova GS, Rutkowska-Gorczyca M. A review on properties of electrodeposited nickel composite coatings: Ni-Al_2O_3, Ni-SiC, Ni-ZrO_2, Ni-TiO_2 and Ni-WC. Materials. 2024; 17(23):5715. https://doi.org/10.3390/ma17235715 PMid:39685150 PMCid:PMC11642598
31. Ünal E, Yaşar A, Karahan İH. Investigation of the properties of Ni-B alloy nanocomposite coatings reinforced with TiC particles electrodeposited at different current densities. J Mater Eng Perform. 2026; 35:7324-7343. https://doi.org/10.1007/s11665-025-12244-9
32. Zhang Y, Gu F, Tian W, Cui H, Zhang H, Ni Q. Enhanced wear and corrosion resistance by GO@SiO_2 *in-situ* polymerized nanoparticles in electrodeposited nickel-base composite coatings. Surf Coat Technol. 2026; 520:133022. https://doi.org/10.1016/j.surfcoat.2025.133022
33. Raghavendra CR, Basavarajappa S, Sogalad I. Electrodeposition of Ni-nano composite coatings: A review. Inorg Nano-Met Chem. 2018; 48(12):583-598. https://doi.org/10.1080/24701556.2019.1567537
34. Saini A, Singh G, Mehta S, Singh H, Dixit S. A review on mechanical behaviour of electrodeposited Ni-composite coatings. Int J Interact Des Manuf. 2023; 17:2247-2258. https://doi.org/10.1007/s12008-022-00969-z
35. Mahidashti Z, Aliofkhazraei M, Lotfi N. Review of nickel-based electrodeposited tribo-coatings. Trans Indian Inst Met. 2018; 71:257-295. https://doi.org/10.1007/s12666-017-1175-x
36. Priyadarshi P, Katiyar PK, Maurya R. A review on mechanical, tribological and electrochemical performance of ceramic particle-reinforced Ni-based electrodeposited composite coatings. J Mater Sci. 2022; 57:19179-19211. https://doi.org/10.1007/s10853-022-07809-1
37. Sajjadnejad M, Haghshenas SMS, Targhi VT, Setoudeh N, Hadipour A, Moghanian A, *et al*. Wear behavior of alkaline pulsed electrodeposited nickel composite coatings reinforced by ZnO nanoparticles. Wear. 2021; 468-469:203591. https://doi.org/10.1016/j.wear.2020.203591
38. Duan XL, Yuan DR, Yu FP. Cation distribution in Co-doped $ZnAl_2O_4$ nanoparticles studied by XPS and ^{27}Al solid-state NMR. Inorg Chem. 2011; 50:5460-5467. https://doi.org/10.1021/ic200433r PMid:21612229
39. Ianoș R, Borcănescu S, Lazău R. Large surface area $ZnAl_2O_4$ powders prepared by a modified combustion technique.

Chem Eng J. 2014; 240:260-263. https://doi.org/10.1016/j.cej.2013.11.082

40. Foletto EL, Battiston S, Marimon JS, Bassaco MM, Pereira LSF *et al*. Synthesis of $ZnAl_2O_4$ nanoparticles by different routes and the effect of pore size on the photocatalytic process. Microporous Mesoporous Mater. 2012; 163:29-33. https://doi.org/10.1016/j.micromeso.2012.06.039
41. Aruna ST, Mukasyan AS. Combustion synthesis and nanomaterials. Curr Opin Solid State Mater Sci. 2008; 12:44-50. https://doi.org/10.1016/j.cossms.2008.12.002
42. Maniam KK, Paul S. Progress in electrodeposition of zinc and zinc nickel alloys using ionic liquids. Appl Sci. 2020; 10(15): 5321. https://doi.org/10.3390/app10155321

Author Contribution

S. Venkatavardan: Investigation, Data Curation, Formal analysis, Validation. S.T. Aruna: Conceptulization, Methodology, Writing, Supervision, Project Administration.